arXiv:1603.02083v3 [nucl-ex] 17 Jun 2016

Fluctuations in Charged Particle Multiplicities in Relativistic Heavy-Ion Collisions

Maitreyee Mukherjee, Sumit Basu, Subikash Choudhury & Tapan K. Nayak

Variable Energy Cyclotron Centre, Kolkata - 700064, India

E-mail: maitreyee.mukherjee@cern.ch

Abstract.

Multiplicity distributions of charged particles and their event-by-event fluctuations have been compiled for relativistic heavy-ion collisions from the available experimental data at Brookhaven National Laboratory and CERN and also by the use of an event generator. Multiplicity fluctuations are sensitive to QCD phase transition and to the presence of critical point in the QCD phase diagram. In addition, multiplicity fluctuations provide baselines for other event-by-event measurements. Multiplicity fluctuation expressed in terms of the scaled variance of the multiplicity distribution is an intensive quantity, but is sensitive to the volume fluctuation of the system. The importance of the choice of narrow centrality bins and the corrections of centrality bin width effect for controlling volume fluctuations have been discussed. It is observed that the mean and width of the multiplicity distributions monotonically increase as a function of increasing centrality at all collision energies, whereas the multiplicity fluctuations show minimal variations with centrality. The beam energy dependence shows that the multiplicity fluctuations have a slow rise at lower collision energies and remain constant at higher energies.

PACS numbers: 25.75.-q,25.75.Gz,25.75.Nq,12.38.Mh

1. Introduction

One of the basic advantages of the heavy-ion collisions at relativistic energies is the production of large number of particles in each event, which facilitates the event-by-event study of several observables. The major physics goals at these high energies are to understand the nature of phase transition from normal hadronic matter to a phase of quark-gluon plasma (QGP). This topic has been of tremendous interest over last four decades, both in terms of theoretical studies and large scale experiments. Dedicated experiments have been performed at the Alternating Gradient Synchrotron (AGS) and Relativistic Heavy Ion Collider (RHIC) at Brookhaven National Laboratory, and the Super Proton Synchrotron (SPS) and the Large Hadron Collider (LHC) at CERN to search as well as study the QGP phase. These experiments explore the QCD phase transition. The fluctuations of experimentally accessible quantities, such

as particle multiplicity, mean transverse momentum, temperature, particle ratios, and other global observables are related to the thermodynamic properties of the system, such as the entropy, specific heat, chemical potential and matter compressibility [1, 2, 3, 4]. Fluctuations of these quantities on an event-by-event basis have been used as basic tools for understanding the particle production mechanisms, the nature of the phase transition and critical fluctuations at the QCD phase boundary. A non-monotonic behaviour of the fluctuations as a function of collision centrality and energy may signal the onset of deconfinement, and can be effectively used to probe the critical point in the QCD phase diagram.

Theoretical models, based on lattice QCD, reveal that at vanishing baryon chemical potential (μ_B), the transition from QGP to hadron gas is a crossover, whereas at large μ_B, the phase transition is of first order [5]. Experimental observables at SPS and RHIC energies may point to the onset of deconfinement and a hint of first order phase transition has been indicated [4, 6, 7, 8, 9]. First order phase transitions can lead to large density fluctuations resulting in bubble or droplet formation and hot spots [10, 11, 12, 13, 14], which give rise to large multiplicity fluctuations in a given rapidity interval. The local multiplicity fluctuations have been predicted as a signature of critical hadronisation at RHIC and LHC energies [15]. Measurements at the vanishing $\mu_{\rm B}$ at LHC energies will be important as one can accurately calculate several quantities and their fluctuations.

The multiplicity of produced particles is an important quantity which characterises the system produced in heavy-ion collisions. Consequently, multiplicity and its fluctuation has an effect on all other measurements. Multiplicity fluctuations have been characterised by the scaled variances of the multiplicity distributions, defined as,

$$\omega = \frac{\sigma^2}{\mu}, \tag{1}$$

where μ and σ^2 are the mean and variance of the multiplicity distribution, respectively. Multiplicity fluctuations have been reported by E802 experiment [16] at AGS, WA98 [17], NA49 [18, 19], NA61 [20, 21] and CERES [22] experiments at SPS, and the PHENIX experiment [23] at RHIC. The nature of the multiplicity distributions as a function of centrality and beam energy has been compared to statistical and available model calculations. These results have generated a great deal of interest [23, 24, 25, 26, 27].

Multiplicity fluctuations have contributions from statistical (random) components as well as those which have dynamical (deterministic) origin. The statistical components have contributions from the choice of centrality, fluctuation in impact parameter or number of participants, finite particle multiplicity, effect of limited acceptance of the detectors, fluctuations in the number of primary collisions, effect of rescattering, etc. [2, 14, 28]. The statistical components of the multiplicity fluctuations have direct impact on the fluctuations in other measured quantities. The dynamical part of the fluctuations contain interesting physics associated with the collision, which include time evolution of fluctuations at different stages of the collision, hydrodynamic expansion, hadronisation and freeze-out. In order to extract the dynamical part of the fluctuations,

the contribution to multiplicity from statistical components has to be well understood. We discuss the methods for controlling geometrical fluctuations so that dynamical fluctuations, if present, become more prominent.

In this article, we present a study of charged particle multiplicity fluctuations as a function of centrality and beam-energy for Au+Au collisions for the Beam Energy Scan (BES) energies at RHIC (from $\sqrt{s_{\rm NN}} = 7.7$ GeV to 200 GeV) and Pb+Pb collisions at LHC-energy ($\sqrt{s_{\rm NN}} = 2.76$ TeV) from the available experimental data as well as using different modes of the AMPT (A Multi-Phase Transport) model [29]. In the next section, we present different model settings of AMPT. In section III, we discuss the method of centrality selection for fluctuation studies and the centrality bin width corrections. Multiplicity distributions for all the collision energies are presented in section IV. The results of multiplicity fluctuations are given in section V. A discussion of the results is presented in section VI and the paper is summarised in section VII.

2. AMPT Model

The AMPT model [29, 30, 31] is used as a guidance for obtaining multiplicity distributions and fluctuations wherever the experimental data are not available. The model consists of four main components: the initial conditions, partonic interactions, the conversion from the partonic to the hadronic matter, and hadronic interactions. The model provides two modes: Default and String Melting (SM) [29]. In both the cases, the initial conditions are taken from HIJING [32] with two Wood-Saxon type radial density profile of the colliding nuclei. The multiple scattering among the nucleons of two heavy ion nuclei are governed by the eikonal formalism. In the default mode, energetic partons recombine and hadrons are produced via string fragmentation. The string fragmentation takes place via the Lund string fragmentation function, given by,

$$f(z) \propto \ z^{-1}(1-z)^{a} exp(-\frac{bm_T^2}{z}). \tag{2}$$

Interactions of the produced hadrons are described by A Relativistic Transport model (ART).

In the SM mode, the strings produced from HIJING are decomposed into partons which are fed into the parton cascade along with the minijet partons. The partonic matter coalesce to produce hadrons, and the hadronic interactions are subsequently modelled using ART. While the Default mode describes the collision evolution in terms of strings and minijets followed by string fragmentation, the SM mode includes a fully partonic QGP phase that hadronises through quark coalescence.

For both the modes, Boltzmann equations are solved using Zhang's parton cascade (ZPC) with total parton elastic scattering cross section,

$$\sigma_{gg} = \frac{9\pi\alpha_s^2}{2\mu^2}\frac{1}{1+\mu^2/s} \approx \ \frac{9\pi\alpha_s^2}{2\mu^2}, \tag{3}$$

where α_s is the strong coupling constant, s and t are the Mandelstam variables and μ is the Debye screening mass. Here a, b (fragmentation parameters), α_s and μ are

the key deciding factors for multiplicity yield at particular beam energy. The values are taken as 2.2, 0.5, 0.47 and 1.8 fm^{-1} respectively, corresponding to total parton elastic cross section σ_{gg}=10mb. The mean values of multiplicities are found to match to the experimental data with these tunings. The AMPT model, therefore, provides a convenient way to investigate a variety of observables with the default and SM modes.

3. Centrality selection and centrality bin width correction

The particle production mechanisms are expected to be dependent on the collision energy as well as the centrality of the collision. For most of the analysis, it is important to consider proper centrality window so that fluctuations because of the selection are minimised. Centrality of a collision is characterised by the impact parameter (b) of the collision or equivalently the average number of participating nucleons ($\langle N_{\mathrm{part}} \rangle$). In an experimental scenario it is not possible to access these two quantities, so charged particle multiplicities within a given rapidity range or energy depositions by calorimeters are used. In a model dependent way, the connections of these experimental quantities to b or $\langle N_{\mathrm{part}} \rangle$ are made. This is indeed needed in order to connect any measured quantity with theoretical calculations and to compare them with measurements from other experiments.

In the present study, centrality is selected using the minimum bias distribution of charged particles in the forward pseudorapidity (η) range of $2.0 < |\eta| < 3.0$, and the multiplicity fluctuations are calculated in the central η-range ($|\eta| < 0.5$). Thus the two η-ranges are very distinct and the fluctuation results are unbiased. As an example of centrality selection procedure, in Fig. 1 we present the minimum bias charged particle multiplicity distribution within $2.0 < |\eta| < 3.0$ and transverse momentum (p_{T}) range of $0.2 < p_{\mathrm{T}} < 2.0$ GeV/c in Pb+Pb collisions at $\sqrt{s_{\mathrm{NN}}} = 2.76$ TeV obtained from AMPT model. Depending on the centrality selection requirement, the area under the curve is divided into centrality percentiles. The shaded regions in the figure show selections in 10% centrality cross-section bins (20% bin is shown for most peripheral collisions). For experimental data, centralities are selected by Glauber model fits to the minimum-bias distributions of charged particles [33].

Selection of narrow centrality window is essential for any fluctuation study. For multiplicity fluctuations, this can be understood in terms of a simple participant model. The number of produced particles (N) in a collision depends on $\langle N_{\mathrm{part}} \rangle$ and the number of collisions suffered by each particle. Mathematically this can be expressed as

$$N = \sum_{i=1}^{N_{\mathrm{part}}} n_i \tag{4}$$

where n_i is the number of particles produced in the η-window of the detector by the i^{th}-participant. On an average, the mean value of n_i is the ratio of the average multiplicity in the detector coverage to the average number of participants, i.e., $\langle n \rangle = \langle N \rangle / \langle N_{\mathrm{part}} \rangle$. Thus the fluctuation in particle multiplicity is directly related to the fluctuation in

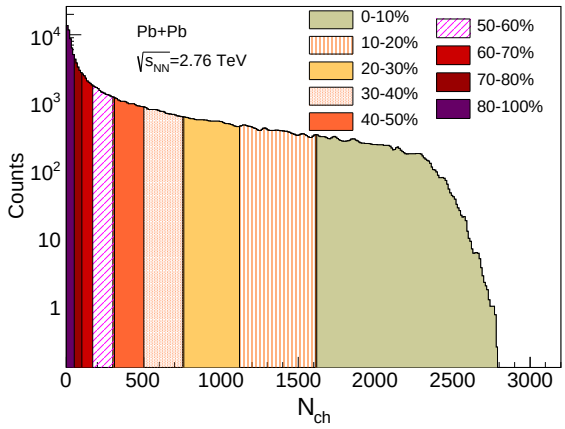

Figure 1. (colour online) An example of centrality selection from minimum-bias distribution of charged particles generated with SM mode of AMPT for Pb+Pb collisions at $\sqrt{s_{\rm NN}} = 2.76$ TeV for $2.0 < |\eta| < 3.0$ and $0.2 < p_{\rm T} < 2.0$ GeV/c.

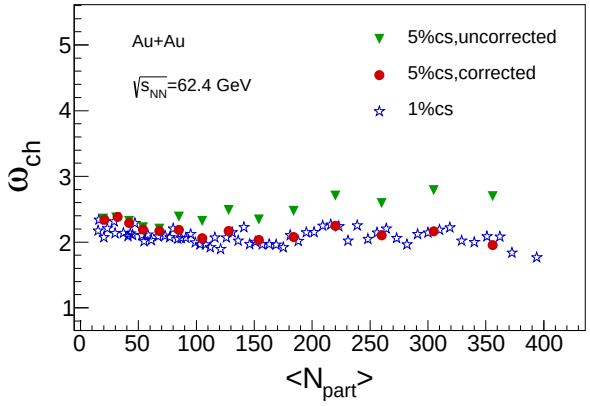

Figure 2. (colour online) Effect of centrality bin width correction on scaled variances (ω_{ch}) is shown for choosing 5% centrality bins. Results for Au+Au collisions at $\sqrt{s_{NN}} = 62.4$ GeV using the default mode of AMPT as a function of $\langle N_{\rm part} \rangle$ shows that after the correction 5% centrality bins are similar to those obtained for 1% centrality bins.

$\langle N_{\rm part} \rangle$. In order to infer dynamical fluctuations arising from various physics processes one has to make sure that the fluctuations in $\langle N_{\rm part} \rangle$ are minimal.

Selection of narrow centrality bins helps to get rid of inherent fluctuations within a centrality bin. The inherent fluctuations are intrinsic fluctuations arising from the difference in geometry even within the centrality bin. A centrality bin scans a range of charged particle multiplicity with different cross sections. This introduces geometrical fluctuations which need to be controlled. Choosing very narrow centrality window minimises the geometrical fluctuations. But it may not be always possible to present the results in such narrow bins, mainly because of lack of statistics and also because

of centrality resolution of detectors used. It is desirable to choose somewhat wider centrality bins, such as 5% or 10% of the total cross sections. But these choices introduce inherent fluctuations which need to be corrected. This is done by taking the weighted average of the observables, such as,

$$X = \frac{\sum_i n_i X_i}{\sum_i n_i}, \tag{5}$$

where the index i runs over each multiplicity bin, X_i represents various moments for the i-th bin, and n_i is the number of events in the i-th multiplicity bin. $\sum_i n_i = N$ is the total number of events in the centrality bin.

This is demonstrated in Fig. 2 in terms of centrality dependence of scaled variance of the multiplicity distributions for Au+Au collisions at $\sqrt{s_{NN}} = 62.4$ GeV with the generated events from the default version of AMPT. Three sets of $\omega_{\rm ch}$ values are presented. The values of $\omega_{\rm ch}$ obtained with 5% centrality bins are much larger compared to the ones with 1% centrality bins. This variation comes because of wide 5% bins. After making the correction of the bin width effect, the fluctuations for the 5% cross section bins reduce by close to $\sim 23\%$ and $\sim 8\%$, respectively for central and peripheral collisions, and almost coincide with that of the 1% cross section bin. No centrality bin width dependence is observed after employing the correction. Thus by choosing narrow bins in centrality and making centrality bin width correction within each centrality window, the volume fluctuations are minimised.

4. Multiplicity distributions

Particle multiplicity distributions for different beam energies and collision centralities help to understand the mechanisms of particle production and constrain various models. Figure 3 shows minimum bias charged particle multiplicity distributions for $|\eta| < 0.5$ and $0.2 < p_{\rm T} < 2.0$ GeV/c in Au+Au collisions at $\sqrt{s_{NN}}$ =19.6 GeV, 27 GeV, 62.4 GeV and 200 GeV, using the default mode of AMPT, and Pb+Pb collisions at $\sqrt{s_{\rm NN}} = 2.76$ TeV using the SM mode of AMPT. As seen from the figure, each distribution gives the maximum extent of the multiplicity for a given collision energy for a given number of events. The maximum extent is larger for larger collision energy.

The minimum bias multiplicity distribution is a convolution of multiplicity distributions with different centrality bins. This is illustrated in Fig. 4 for charged particle multiplicity distributions in case of Pb+Pb collisions at $\sqrt{s_{\rm NN}} = 2.76$ TeV from the SM mode of AMPT model. Minimum bias distribution as well as distributions at different centrality bins are presented.

Width of the multiplicity distribution for a given centrality gives the extent of the fluctuation. Thus the physics origin of the fluctuations are inherent in the width of the multiplicity distributions. One of the ways to understand this to plot the multiplicity distributions within a centrality bin by scaling it to the mean value of multiplicity ($\langle N_{\rm ch} \rangle$). This is presented in Fig. 5 for Au+Au collisions at $\sqrt{s_{\rm NN}} = 62.4$ and 200 GeV using default AMPT and Pb+Pb collisions at $\sqrt{s_{\rm NN}}$ =2.76 TeV using the SM mode

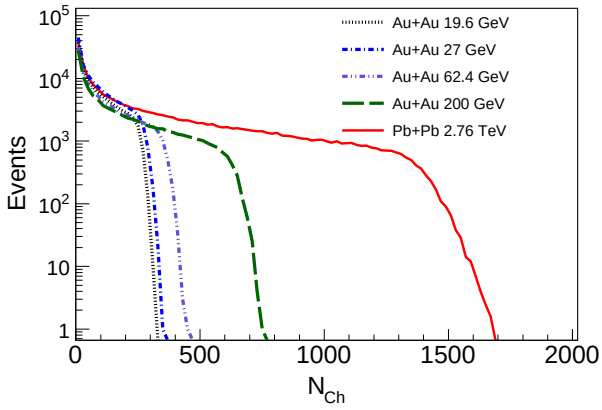

Figure 3. (colour online) Minimum-bias distributions for charged particles for Au+Au collisions at 19.6, 27, 62.4 and 200 GeV using default AMPT model and for Pb+Pb collisions at $\sqrt{s_{\rm NN}} = 2.76$ TeV, obtained using SM version of AMPT within $|\eta| < 0.5$ and $0.2 < p_{\rm T} < 2.0$ GeV/c.

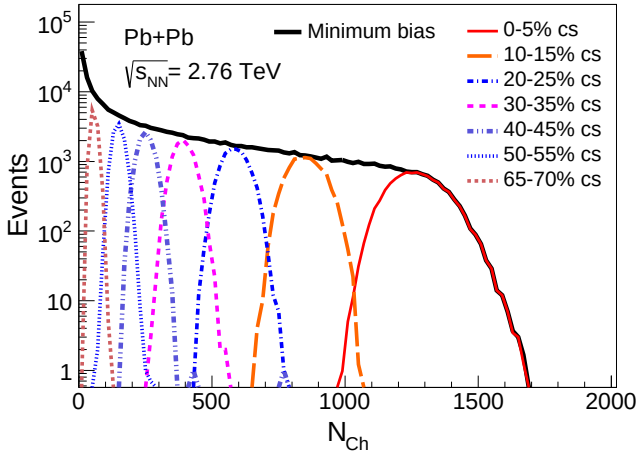

Figure 4. (colour online) Charged particle multiplicity distributions for different centralities for Pb+Pb collisions at $\sqrt{s_{\rm NN}} = 2.76$ TeV using SM mode of AMPT model within $|\eta| < 0.5$ and $0.2 < p_{\rm T} < 2.0$ GeV/c.

of AMPT. The vertical axes are multiplied by different factors for better visibility. In this representation, it is observed that the widths of the distributions are inversely proportional to volume, that is to $\langle N_{\rm ch} \rangle$. Thus the distributions become narrower in going from peripheral to central collisions for all energies. This extensive nature of the representation is avoided by calculating the scaled variance as defined in Eq. (1).

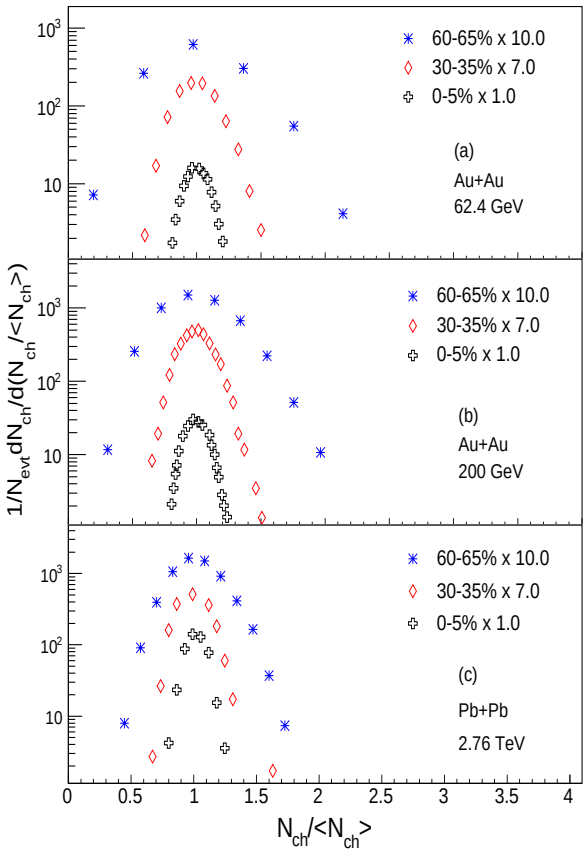

Figure 5. (colour online) Scaled multiplicity distributions of charged particles for centralities corresponding to 0-5%, 30-35% and 60-65% cross sections within $|\eta| < 0.5$ and $0.2 < p_{\rm T} < 2.0$ GeV/c using default AMPT for Au+Au collisions at (a) $\sqrt{s_{\rm NN}} = 62.4$ GeV, (b) $\sqrt{s_{\rm NN}} = 200$ GeV, and using SM mode of AMPT for Pb+Pb collisions at (c) $\sqrt{s_{\rm NN}} = 2.76$ TeV. The charged particle distributions are scaled to the mean values of the distributions.

5. Multiplicity Fluctuations

Multiplicity fluctuations are studied as a function of collision centrality for Au+Au collisions at $\sqrt{s_{\rm NN}}$ = 7.7 GeV,19.6 GeV, 27 GeV, 62.4 GeV, 200 GeV and Pb+Pb collisions for $\sqrt{s_{\rm NN}} = 2.76$ TeV for 5% centrality bins from peripheral to central collisions. For each centrality bin, the multiplicity distributions are corrected using centrality bin width correction method. The AMPT model gives the number of participating nucleons for each centrality bin and so the results are presented as a function of $\langle N_{\rm part} \rangle$. The statistical errors of the μ and σ are calculated using the Delta theorem [34] method. Errors for $\omega_{\rm ch}$ are obtained by propagating the errors on μ and σ. In most cases, statistical errors are observed to be small.

Figure 6 shows the results for μ, σ and $\omega_{\rm ch}$ as a function of $\langle N_{\rm part} \rangle$ for five collision energies. The left panels show the results for events generated using the default mode

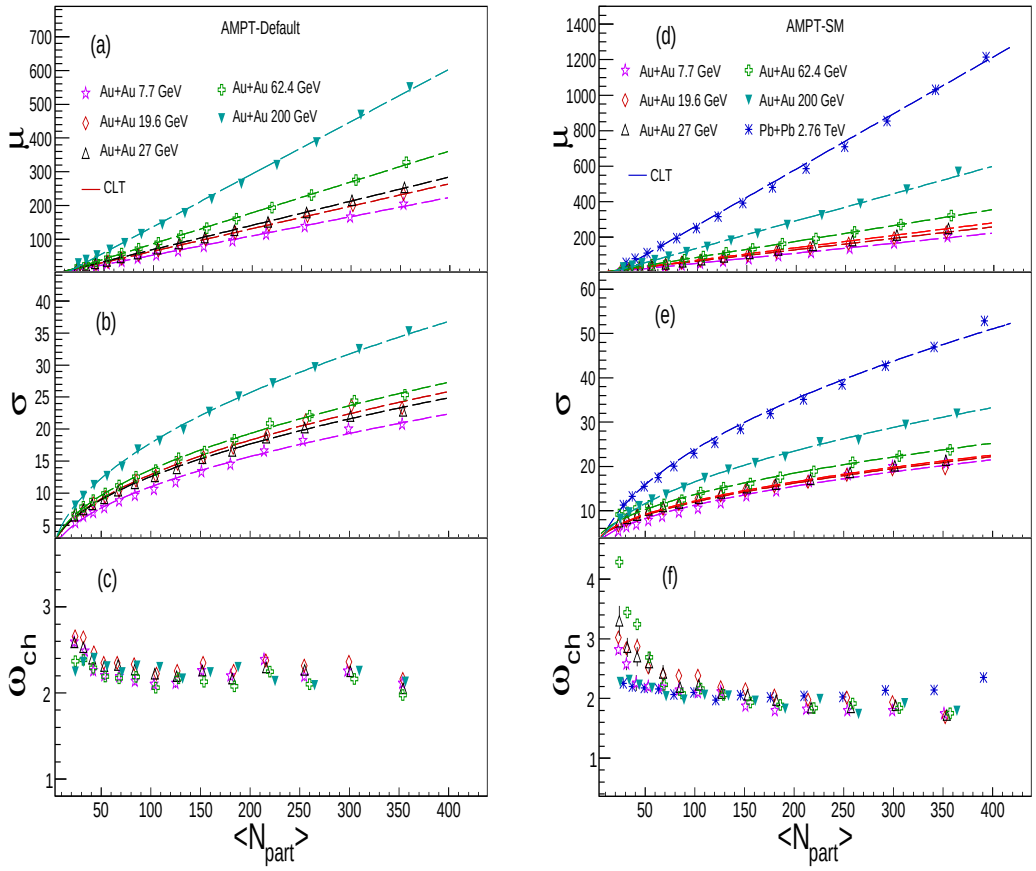

Figure 6. (colour online) Mean, sigma and scaled variance of charged particle multiplicities within $|\eta| < 0.5$ and $0.2 < p_{\rm T} < 2.0$ GeV/c as a function of centrality for a wide range of collision energies. The left panels show the events generated using the default mode of AMPT and the right panels show the corresponding distributions from the SM mode of AMPT. Dashed lines represent fits using the central limit theorem.

of AMPT and the right panels give the results obtained using SM mode of AMPT. For $\sqrt{s_{\rm NN}} = 2.76$ TeV, only the results from the SM mode are presented. It is observed that for all collision energies, μ and σ increase smoothly in going from peripheral to central collisions for all energies. The centrality evolution of the moments can be understood by the Central Limit Theorem (CLT) according to which,

$$\mu \propto \langle N_{\rm part} \rangle \tag{6}$$

$$\sigma \propto \sqrt{\langle N_{\rm part} \rangle}. \tag{7}$$

It is to be noted that $\langle N_{\rm part} \rangle$ is proportional to the volume of the system, and so $\omega_{\rm ch}$ is a volume independent term. In Figure 6, μ and σ are fitted with respective CLT-form as in the above expressions with the constant of proportionality as free parameter. The CLT curves are superimposed on the AMPT points. The centrality evolution of the moments follow the trend of the CLT at all energies. Deviations to CLT fits are seen for central collisions at the highest energy considered.

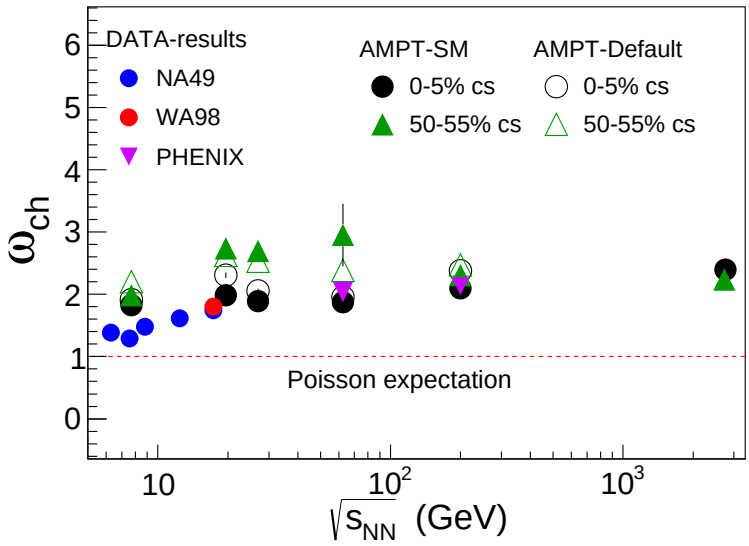

Figure 7. (colour online) Beam-energy dependence of scaled variance ($\omega_{\rm ch}$) of charged particle multiplicity distribution for central (0-5% cross section) and peripheral (50-55% of cross section) collisions as a function of collision energy for available experimental data and for events generated using two modes of AMPT model.

The bottom panels of Fig. 6 show the scaled variances ($\omega_{\rm ch}$) as a function of centrality for different collision energies. The results are similar for both default and SM modes of AMPT. At low collision energies, $\omega_{\rm ch}$ show a drop in going from most peripheral collisions after which the values remain unchanged. At higher energies, $\omega_{\rm ch}$ remain rather constant as a function of centrality.

Beam-energy dependences of the multiplicity fluctuations have been studied by combining results from available experimental data with AMPT model calculations. Experimental results for heavy-ion collisions are available for WA98 [17] and NA49 [18, 19] experiments at CERN SPS and PHENIX [23] experiment at RHIC. Since these experimental results are presented for different detector acceptances, these have to be scaled to a common acceptance in order to present in the same figure. The available results are scaled for $\Delta\eta < 1$ using the prescription given Ref. [23]. If $\omega_{\rm acc1}$ represents the measured scaled variance and $\omega_{\rm acc2}$ is the scaled variance within $\Delta\eta < 1$, then we have [23],

$$\omega_{\rm acc2} = 1 + f_{\rm acc}(\omega_{\rm acc1} - 1) \tag{8}$$

where,

$$f_{\rm acc} = \frac{\mu_{\rm acc2}}{\mu_{\rm acc1}}. \tag{9}$$

The values of $\omega_{\rm acc2}$ have been calculated from the data provided by the experiments. Fig. 7 shows the values of $\omega_{\rm ch}$ for central collisions for WA98, NA49 and PHENIX experiments. The results for $\omega_{\rm ch}$ are also presented for two different centralities (0-5%

and 50-55% of total cross section) using the default and SM modes of AMPT. A slow rise in $\omega_{\rm ch}$ has been observed from low to high collision energy and then remaining constant at higher energies. The AMPT results overestimate those of NA49 experimental data, but are close to those of WA98 and PHENIX data. These values are larger compared to the Poisson expectations.

6. Discussions

Collision energy dependence of fluctuations of charged particle multiplicity, presented in Fig. 7 does not show any non-monotonic behaviour for the AMPT results as well as for experimental data. The experimental data and AMPT results are rather close to each other. Non-monotonic behaviour is not expected from the AMPT event generator as it does not contain any physics specific to phase transition and critical behaviour. The absence of non-monotonic behaviour in the experimental data point to the absence of critical phenomenon for the systems studied at SPS and RHIC. In addition, the observed fluctuations in charged particles may be affected by the evolution of fluctuation during the early collision time to freeze-out. More data for Beam Energy Scan (BES) energies at RHIC are needed to make any definitive conclusion on the critical behaviour. The results presented using the AMPT event generator provide baselines for these studies at BES energies and for collisions at the Large Hadron Collider (LHC).

Multiplicity fluctuations arise from several known sources such as, fluctuations in the number of sources producing multiplicity, fluctuations in the number of particles produced in each source, detector-acceptance, resonance decays, etc. If particles are produced independently, one gets $\omega_{ch} = 1$. But as we move to higher energies, the non-statistical fluctuations increase and automatically contribute to the increased value of the fluctuation as discussed in Ref. [38]. Various studies have been reported in the literature in order to explain the values for multiplicity fluctuations expressed in terms of the scaled variances [7, 10, 14, 23, 37]. Ref. [37] gives a prediction for the values of scaled variance in grand canonical ensemble (GCE), canonical ensemble (CE) and micro canonical ensemble (MCE) using the hadron resonance gas model at chemical freeze-out for the central heavy-ion collisions for a wide collision energy range. According to these calculations, we get a value for ω_{ch} between 1.4 to 1.64 for GCE, 1.06 to 1.64 for CE, and 0.534 to 0.619 for MCE. At higher energies, the scaled variance is predicted to be similar for CE and GCE. In Ref. [18], it is observed that, the values for the scaled variance from NA49 experiment is better described by MCE. Results presented in Fig. 7 are close to the GCE description for higher collision energies.

An estimation for the multiplicity fluctuation can be made in the light of the participant model, where the nucleus-nucleus collisions are assumed to be superposition of nucleon-nucleon interactions (as described in Ref. [10]). Here, the total multiplicity fluctuation has contributions due to fluctuations in $N_{\rm part}$ and also due to the fluctuation in the number of particles produced per participant. In this formulation, $\omega_{\rm ch}$ can be

expressed as,

$$\omega_{\rm ch} = \omega_{\rm n} + \langle n \rangle \omega_{N_{\rm part}} \tag{10}$$

where, n is the number of charged particles produced per participant, $\omega_{\rm n}$ denotes fluctuations in n, and $\omega_{N_{\rm part}}$ is the fluctuation in $N_{\rm part}$. The value of $\omega_{\rm n}$ has a strong dependence on acceptance. The fluctuations in the number of accepted particles (n) out of the total number of produced particles (m) can be calculated by assuming that the distribution of n follows a binomial distribution. This is given as [10, 17],

$$\omega_{\rm n} = 1 - f + f\omega_{\rm m}, \tag{11}$$

where f is the fraction of particles accepted. The values of f are obtained from the published proton-proton collision data for total number of charged particles and number of charged particles in mid-rapidity over the energy range considered [39, 40, 41]. $\omega_{\rm m}$ is calculated from the total number of charged particles using the formulation given in Ref. [17]. Using these, we obtain the values of $\omega_{\rm n}$ as a function of collision energy. The values of $\omega_{\rm n}$ vary within 0.98 to 2.0 corresponding to $\sqrt{s_{\rm NN}}$ =7.7 GeV to 2.76 TeV. These values match with those reported for SPS collisions [17, 38]. By using the values of $\omega_{\rm n}$ in Eqn. (10), we find that $\omega_{\rm ch}$ from the statistical model calculations are close to those of the AMPT results presented in Fig. 7. We observe that the values of $\omega_{\rm n}$ has a major contribution to $\omega_{\rm ch}$.

7. Summary

We have presented a comprehensive study on the fluctuations of charged particle multiplicity at mid-rapidity as a function of collision centrality and beam-energy. We have studied the multiplicity distributions of produced charged particles and their event-by-event fluctuations for heavy-ion collisions using the available experimental data and AMPT model calculations. We have demonstrated the importance of the choice of centrality selection and a detailed discussion on the bin-width effect and its remedy have been presented. The scaled variance, ω_{ch} is constructed in such a way that statistical fluctuations give the same result at any multiplicity. Thus, it has negligible dependence on centrality and beam energy. Comparison with experimental data and AMPT results has been presented after a proper rescaling to consider the difference in the geometrical acceptance. We observe that the mean and width of the multiplicity distributions monotonically increase as a function of increasing centrality at all collision energies, whereas $\omega_{\rm ch}$ shows minimal variation with centrality. The beam energy dependence shows that $\omega_{\rm ch}$ has a slow rise at lower collision energies and remain constant at higher energies. $\omega_{\rm ch}$ at higher energies and central collisions are found to be $\sim$2 within the limits of statistical precision. The model calculations exhibit good agreement with the results from WA98, NA49 and PHENIX experiments. The values of the $\omega_{\rm ch}$ are found to be consistent with the participant model calculations, where charged particle fluctuation is considered as a sum of particle number fluctuation from each source and fluctuation in number of sources. We observe that the fluctuation in number of particles produced

per participant has a dominant effect on $\omega_{\rm ch}$. Both data and model calculations have no distinct signature of any non-monotonic variation. Our study offers a baseline for the future endeavour to pursue research on particle multiplicity fluctuations at Facility for Antiproton and Ion Research (FAIR), RHIC and LHC energies.

Acknowledgement

This research used resources of the LHC Grid computing facility at Variable Energy Cyclotron Centre, Kolkata.

References

[1] M. A. Stephanov, K. Rajagopal and E. V. Shuryak, Phys. Rev. Lett. **81**, 4816 (1998).
[2] M.A. Stephanov, K. Rajagopal, and E.V. Shuryak, Phys. Rev. **D 60**, 114028 (1999).
[3] M. A. Stephanov, Prog. Theor. Phys. Suppl. **153**, 139 (2004); Int. J. Mod. Phys. **A 20**, 4387 (2005).
[4] M. Gazdzicki, M.I. Gorenstein and S. Mrowczynski, Phys. Lett. **B 585**, 115 (2004).
[5] Y. Aoki et al., Nature **443**, 675 (2006).
[6] Marek Gazdzicki, Mark Gorenstein and Peter Seyboth, Acta Phys. Polon. **B 42** 307 (2011).
[7] M. Gazdzicki and P. Seyboth, arXiv:1506.08141v2 [nucl-ex].
[8] B. Mohanty, J. Alam, S. Sarkar, T.K. Nayak and B.K. Nandi, Phys. Rev. **C 68**, 021901 (2003).
[9] M.M. Aggarwal *et al.* (STAR Collaboration) e-Print: arXiv:1007.2613 [nucl-ex].
[10] H. Heiselberg, Phys. Rept. **351** 161 (2001).
[11] L. van Hove, Z. Phys. **C 21**, 93 (1984).
[12] J.I. Kapusta and A.P. Vischer, Phys. Rev. **C52**, 2725 (1995).
[13] A. Bialas, Phys. Lett. **B 532**, 249 (2002).
[14] G. Baym and H. Heiselberg, Phys. Lett. **B 469**, 7 (1999).
[15] R. Hwa and C.B. Yang, Phys. Rev. **C 85**, 044914 (2012).
[16] T. Abbott *et al.* (E-802 Collaboration), Phys. Rev. **C 52**, 2663 (1995).
[17] M. M. Aggarwal *et al.* (WA98 Collaboration) Phys. Rev. **C 65**, 054912 (2002).
[18] C. Alt. *et al.* (NA49 Collaboration), Phys. Rev. **C 78**, 034914 (2008).
[19] M. Rybczynskil *et al.* (NA49 Collaboration), Jour. of Phys.: Conference Series **5**, 74 (2005).
[20] T. Czopowicz (NA61/SHINE Collaboration), arXiv:1503.01619 [nucl-ex].
[21] A. Aduszkiewicz et al. [NA61/SHINE Collaboration], arXiv:1510.00163 [hep-ex].
[22] H. Sako. *et al.*, (CERES Collaboration), J.Phys. G30 (2004) S1371-S1376.
[23] A. Adare *et al.* (PHENIX Collaboration) Phys. Rev. C 78, 044902 (2008), arXiv: 0805.1521[nucl-ex] (2008).
[24] V. V. Begun, M. I. Gorenstein, A. P. Kostyuk and O. S. Zozulya, Phys. Rev. **C 71**, 054904 (2005).
[25] S. Jeon and V. Koch, arXiv:hep-ph/0304012.
[26] V. V. Begun, M. Gazdzicki, M. I. Gorenstein and O. S. Zozulya, Phys. Rev. **C 70**, 034901 (2004).
[27] F. Becattini, A. Keranen, L. Ferroni and T. Gabbriellini, Phys. Rev. **C 72** 064904 (2005).
[28] R.C. Hwa, Phys. Lett. **B201** 165 (1988).
[29] Z.-W. Lin, C.M. Ko, B.-A. Li, B. Zhang, S. Pal, Phys. Rev. **C 72**, 064901 (2005).
[30] Z.W. Lin *et al.*, Phys. Rev. **C 64**, 011902 (2001).
[31] B. Zhang *et al.*, Phys. Rev. **C 61**, 067901 (2000).
[32] X.-N. Wang, M. Gyulassy, Phys. Rev. **D 44**, 3501 (1991).
[33] B. Abelev *et al.* (ALICE Collaboration), Phys. Rev. **C 88**, 044909 (2013).
[34] X. Luo, J. Phys. G : Nucl. Part. Phys. **39** 025008 (2012), arXiv:1109.0593v1 (2012).
[35] M. Floris *et al* (ALICE collaboration), Nucl. Phys. **A 910**, 343 (2013).
[36] M. L. Miller, K. Reygers, S. J. Sanders, and P. Steinberg, Annu. Rev. Nucl. Part. Sci. **57**, 205 (2007).

[37] V. Begun, M. Gazdzicki, M.Gorenstein, M.Hauer, V.Konchakovski, and B.Lungwitz , arxiv:nucl-th/0611075 (2007).
[38] G.V.Danilov and E.V.Shuryak, arxiv:nucl-th/9908027 (1999).
[39] B.B. Back *et al.* (PHOBOS Collaboration), arXiv:nucl-ex/0301017.
[40] K. Aamodt *et al.* (ALICE Collaboration), Phys. Rev. Lett. **106** 032301 (2011).
[41] S. Chatrchyan *et al.* (CMS Collaboration) and G. Antchev *et al.* (TOTEM Collaboration), Eur. Phy. Jour. **C74** 2053 (2014).